Colloids and Surfaces A: Physicochem. Eng. Aspects 353 (2010) 238–244

Contents lists available at ScienceDirect

Colloids and Surfaces A: Physicochemical and Engineering Aspects

journal homepage: www.elsevier.com/locate/colsurfa

Phosphate adsorbed on Fe(III) modified montmorillonite: Surface complexation studied by ATR-FTIR spectroscopy

Laura Borgnino[a,*], Carla E. Giacomelli[a], Marcelo J. Avena[b], Carlos P. De Pauli[a]

[a] INFIQC, Departamento de Fisicoquímica, Facultad de Ciencias Químicas, Universidad Nacional de Córdoba, Ciudad Universitaria, 5000, Córdoba, Argentina
[b] INQUISUR Departamento de Química, Universidad Nacional del Sur. Av. Alem 1253, 8000 Bahía Blanca, Argentina

ARTICLE INFO

Article history:
Received 10 August 2009
Received in revised form 5 November 2009
Accepted 9 November 2009
Available online 13 November 2009

Keywords:
Phosphate
Adsorption
Electrophoretic mobility
ATR-FTIR
Surface complexes
Fe(III)-montmorillonite

ABSTRACT

This work is aimed at determining phosphate speciation at the Fe(III)-modified montmorillonite/aqueous solution interface by attenuated total reflectance (ATR-FTIR) spectroscopy. IR spectra are analyzed by second derivative and Fourier self-deconvolution procedures to reveal the number and positions of overlapped bands related to phosphate surface complexes. Experiments are conducted at pH 4.5, 7.0 and 9.0 in order to determine the effects of changing pH on the surface speciation. The molecular view offered by the ATR-FTIR measurements is complemented by macroscopic adsorption data, such as adsorption isotherms and electrophoretic mobilities. The ATR-FTIR spectral analyses reveal the existence of two inner-sphere complexes when phosphate adsorbs on modified montmorillonite, as also suggested from macroscopic adsorption data. The complex coordination depends on the pH. At pH 4.5, both complexes present C_{2V} symmetry or lower. On the other hand, at pH 7.0 and 9.0 one of them is also C_{2V} or lower while the other one presents C_{3V} symmetry. Adsorbed phosphate is not associated with montmorillonite itself but with Fe(III) (hydr)oxides coatings. Therefore, the clay acts as a carrier or support of the Fe(III)-(hydr)oxides, and these coatings are responsible for phosphate adsorption.

1. Introduction

The geochemical behavior of phosphate has been the subject of numerous studies in various disciplines [1–5]. The interest stems from the fact that phosphate is essential for plant growth in soils and it is the nutrient that usually limits algae growth and eutrophication in surface water [6,7]. Eutrophication as well as the overgrowth of cyanobacteria due to the excess of phosphate in recreational, industrial, and drinking water could greatly threaten human and ecological health [8,9]. Therefore, in order to design effective remediation strategies for reducing negative impacts on aquatic/terrestrial environments, it is necessary to understand the fate and transport of phosphate in soil/water and sediment/water environments. For this reason, phosphate adsorption on natural adsorbent has been widely studied during the past years [10–16]. These research works have well established that phosphate has a relatively strong affinity for metal (hydr)oxides, especially those of iron and aluminum [12–14,17,18], and that the adsorbed amount strongly depends on pH [3,12]. Furthermore, spectroscopy studies have shown that phosphate adsorbs on Fe(III) (hydr)oxides through the formation of different inner-sphere surface complexes [19–24]. However, the adsorption on aquatic/terrestrial environments may be different from that inferred directly by working with metal (hydr)oxides, since phosphate species not only adsorbed on pure (hydr)oxides, but also on clays that are coated or modified with metal (hydr)oxides [4,25,26].

Most clay minerals carry a net negative charge within their structure that is balanced by exchangeable cations. This negative charge gives important cation adsorption and cation exchange properties to clays, which have been widely used to remove metal cations, organic pollutants and bacteria from water and wastewater [27–29]. Such negative structural charge impedes, however, electrostatic attraction between clay particles and inorganic anions, as phosphate. In addition, the relatively stable siloxane groups located on the basal surfaces of clays do not appear to react appreciably with phosphate to produce surface complexes by ligand exchange processes [30]. As a result, pure phyllosilicate clays have a very low affinity for phosphate [31], and their phosphate adsorption capacity is negligible compared to that of pure Al or Fe (hydr)oxides [3,16,21].

The phosphate adsorption capacity of clays can be readily increased by modifying the clays with Fe or Al hydroxylated species. These metal (hydr)oxide modified clays represent a suitable model to study the adsorption capabilities of natural occurring systems. Borgnino et al. [31], for example, showed that the phosphate adsorption capacity of a pure montmorillonite was significantly

* Corresponding author. Fax: +54 351 4334188.
E-mail addresses: borgnino@mail.fcq.unc.edu.ar (L. Borgnino), giacomel@mail.fcq.unc.edu.ar (C.E. Giacomelli), mavena@uns.edu.ar (M.J. Avena), depauli@mail.fcq.unc.edu.ar (C.P. De Pauli).

0927-7757/$ – see front matter © 2009 Elsevier B.V. All rights reserved.
doi:10.1016/j.colsurfa.2009.11.022

enhanced by modifying the clay with Fe(III). Phosphate adsorption on two different Fe(III)-modified montmorillonites with different Fe(III) contents was 16 and 55 times larger than that of a sodium montmorillonite [31]. Kasama et al. [32] investigated phosphate adsorption on Al-pillared smectites and found that the maximum adsorbed amount of phosphate was two orders of magnitude higher on Al-pillared samples when compared to smectites without pillars. Zhu et al. [33] studied phosphate adsorption on hydroxyaluminum- and hydroxyiron-montmorillonite complexes and they found that an increase in Fe contents could enhance the phosphate adsorption capacity. The adsorption of metals and other anions, such as arsenate, on modified phyllosilicate, clays minerals and amorphous aluminosilicates has been also reported in the literature [34–37].

All the mentioned studies were mainly focused on determining the phosphate adsorption capacity of modified montmorillonites. However, no studies were directed to identify the adsorbed phosphate species. An identification of them will allow a better understanding of the adsorptive properties of modified clays and will give new insights into the role that iron modification plays in the fate and transport of phosphate in the environment.

The aim of this work is to perform phosphate adsorption on Fe(III)-modified montmorillonite and to determine phosphate speciation at the solid/liquid interface by using attenuated total reflectance (ATR-FTIR) spectroscopy. The capabilities of infrared spectroscopy have been applied to study the adsorption mechanism of phosphate, carbonate, sulfate, and various inorganic ligand on metal (hydr)oxides, and to characterize the surface complexes sorbed onto those mineral surfaces [38]. In the present study, the IR spectra are analyzed by second derivative and Fourier self-deconvolution procedures to reveal the number and positions of overlapped bands related to phosphate surface complexes. In addition, the spectral analyses allow comparing the results obtained on Fe(III)-modified montmorillonite to previous IR studies performed on different Fe(III) (hydr)oxides [19–23]. Experiments are conducted at different pH values in order to determine the effects of changing pH on the surface speciation. The molecular view offered by the ATR-FTIR measurements is complemented by macroscopic adsorption data, such as adsorption isotherms and electrophoretic mobilities.

2. Materials

All solutions were prepared from analytical reagent grade chemicals and purified water (Milli-Q system). The temperature was maintained at $26 \pm 1^\circ$ in all the experiments.

The montmorillonite used in this study was obtained from Cerro Banderita (province of Neuquén, Argentina). Particles with a diameter <2 μm were obtained by sedimentation and saturated with Na^+ by treating the clay suspension with 1 M NaCl. The sodium-exchanged clay (Na-M) has a cation exchange capacity of 91.7 meq/100 g and a specific surface area of 833 $m^2\,g^{-1}$, measured by the methylene blue adsorption method [39].

The synthesis procedure and the characterization of the Fe(III)-modified montmorillonite (Fe-M) was described elsewhere [31]. Briefly, 550 mL of a 0.01 M Fe(III) nitrate solution (pH 3.5) were mixed with 250 mL of a 2.2% Na-M dispersion in water at the same pH with vigorous stirring during 2 h. Then, a NaOH solution was added dropwise up to pH 9.0 and the dispersion was stirred for other 3 h. Finally, the solid was washed with water and dried at 60 °C during 3 days. The resulting solid has an iron content of 77.3 mg g^{-1} and a specific surface area of 567 $m^2\,g^{-1}$, measured by the methylene blue adsorption method. More than 60% of the total Fe(III) in this sample corresponds to interlayer/sorbed Fe(III). The remaining fraction was already present in Na-M (structural Fe) [31].

Powder X-ray diffraction (XRD) patterns were recorded on a Philips XïPert PRO X-ray diffractometer, using CuK_α radiation (30 kV to 15 mA). XRD data were obtained in the 2θ range from 4 to 15° (step size: 0.01; 4 seg/step). The reflection assignments were done using the software XïPert HighScore, installed on the X-ray diffractometer.

3. Methods

3.1. Batch phosphate adsorption studies

Phosphate adsorption isotherms were measured in batch experiment at pH 4.5, 7.0, and 9.0, in order to determine the effects of changing pH on the surface speciation. For each data point 1 g of solid was suspended in 40 mL of a 0.01 M NaCl solution and the pH of this mixture was adjusted to either 4.5, 7.0 or 9.0 by addition of a HCl or NaOH solution. A well-known volume of a 0.01 M phosphate solution, prepared in 0.01 M NaCl and having the same pH than the suspension was then added. Any change in pH after the mixing was readjusted by adding either HCl or NaOH solutions. After 24 h of equilibration, the pH was registered, the suspension was centrifuged, the supernatant analyzed for phosphate concentration following the method proposed by Murphy and Riley [40] and the adsorbed amount calculated.

3.2. Electrophoretic mobility (EM) measurements

Electrophoretic mobility measurements were carried out using a Rank Brothers Mark II electrophoresis apparatus equipped with a cylindrical cell. Dispersions of approximately 0.02 g L^{-1} of Na-M or Fe-M suspension were prepared by dispersing the clay sample in 0.01 M NaCl. The pH of the suspension was raised to approximately 9.0 with NaOH and an EM measurement was carried out. After that, the pH was slightly decreased with HCl and a new EM measurement performed. This procedure was continued until the pH was around 3.5. Each reported data is the average of the reading of 20 individual particles. To study the effect of phosphate on the EM, measurements at different pH were carried out to solids suspended in 0.01 M NaCl in the presence of 0.01 M phosphate.

3.3. ATR-FTIR experiments

ATR-FTIR spectra were recorded with a Nicolet Magna 560 FTIR apparatus equipped with a DTGS detector and a horizontal trough Ge crystal as the internal reflection element (45° incidence angle; 0.67 μm penetration depths at 2000 cm^{-1}; 12 reflections). Each spectrum was obtained as the average of 1000 individual scans using a 2 cm^{-1} resolution. For these measurements, a stock Fe-M dispersion (10 g L^{-1}) was prepared by dispersing the solid in a 0.01 M NaCl solution. The resulting dispersion was shaken during one hour and the pH adjusted to the desired value (4.5, 7.0 or 9.0). Several drops of this dispersion were placed on top of the Ge crystal and let dry under vacuum overnight in order to form a dried Fe-M film. The film was then rinsed with water to eliminate the loosely attached particles. Then, the film was covered with 0.01 M NaCl solution at the desired pH in order to record spectrum 2 (see Section 3.3.1). After withdrawing the electrolyte solution, a phosphate solution prepared in 0.01 M NaCl at the same pH was added and let equilibrate during 3 hours before recording spectrum 3 (see Section 3.3.1). The concentration of the added phosphate solution (always in the 0.4–0.9 mM range) at a given pH was adjusted in such a way that the phosphate adsorbed amount corresponds to the plateau value of the adsorption isotherms.

3.3.1. Spectral analysis

The following spectra were recorded: spectrum 1, ATR-Ge crystal in air (background); spectrum 2, ATR-Ge crystal + Fe-M film + NaCl solution; spectrum 3, ATR-Ge crystal + Fe-M

film + phosphate in NaCl solution. In order to obtain IR data of adsorbed phosphate species, spectrum 2 was finally subtracted from spectrum 3. This subtraction allows to eliminate the strong Si–O vibration band (~1040 cm^{-1}) of the montmorillonite structure, which interferes with IR bands associated with the ν(P–O) signals (900–1200 cm^{-1}). It also allows to partially removing the interferences caused by the (H–O–H) absorption band in the spectral region between 900 and 800 cm^{-1} [41,42].

The spectra resulting from the subtraction were analyzed using second derivative (SD) and Fourier self-deconvolution (FSD) procedures. These spectral analyses were applied with the algorithms provided with the FTIR spectrophotometer (OMNIC E.S.P. 5.1 software). Both mathematical methods allow to reveal the number and the position of overlapping bands (Appendix B see supporting material, Note I) [43–45]. Before using these mathematical procedures, the spectra were smoothed (Savitsky–Golay, 5 points window). The FSD method was applied using a triangular apodization and, depending on the signal to noise ratios, the bandwidths were set between 65 and 103 cm^{-1} while the enhancement parameter was fixed in 2.5.

Additional experiments were performed without the Fe-M film to record the spectra of dissolved phosphate species in NaCl solution at the studied pH values. For these experiments 0.01 M phosphate solutions were used. The contribution from aqueous phosphate species in the ATR-IR spectrum becomes visible above noise level at solution concentration of approximately 700 μM [23]. In our adsorption experiments, this contribution was negligible because phosphate concentration in the used solutions was always lower than 500 μM.

4. Results and discussion

4.1. General characterization and adsorption studies

Fig. 1 shows the phosphate adsorption isotherms in 0.01 M NaCl at different pH values. Lines in the figure were drawn only to serve as guides to the eyes. The adsorbed amount per unit area was calculated using the specific surface area measured by the methylene blue adsorption method, instead of the single-point N_2 method used in a previous study [31]. The first method allows obtaining a value that is more representative of the actual surface area of clays samples, and hence it is preferred. Phosphate adsorption increases as the pH decreases, which is consistent with other anion adsorption studies [46–48]. The general adsorption behavior, i.e. extent of adsorption and its pH dependency, is comparable to the behavior on goethite and ferrihydrite [3,21].

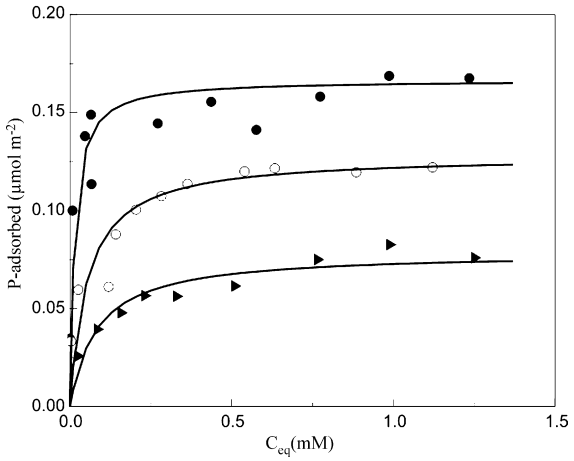

Fig. 1. Phosphate adsorption isotherms on Fe-M at pH 4.5 (solid circles), 7.0 (open circles) and 9.0 (solid triangles). Lines are drawn only to serve as guides to the eyes.

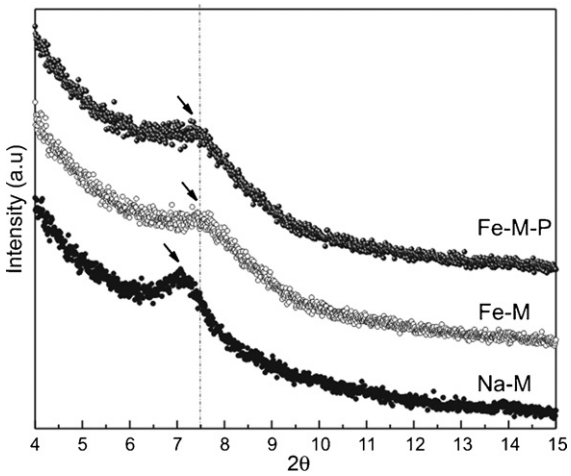

Fig. 2. XRD pattern of a Na-M, Fe-M and Fe-M-P samples. Arrows indicate the 0 0 1 reflection.

In a previous work Borgnino et al. [31] show that the phosphate adsorption capacity of Fe-M at pH 4.5 is 16 times larger than that of Na-M. Although data are not show here, it is worth mentioning that the adsorption per unit area increases as the iron content raises. This greater adsorption capacity is attributed to the presence of interlayer/sorbed Fe(III), which is the main iron component of the studied sample [31]. Moreover, Fe-M has a higher adsorption capacity than pure ferrihydrite [21], indicating that the synthesized Fe-M sample presents different surface characteristic from a simple mixture of montmorillonite and ferrihydrite. Therefore, the montmorillonite in the synthesized material behaves as a carrier of the Fe hydr(oxide), which is the responsible for phosphate adsorption.

Fig. 2 shows the XRD patterns of Na-M and Fe-M in the absence (Fe-M) and in the presence (Fe-M-P) of adsorbed phosphate. The pattern obtained for Na-M sample is typical of a sodium-exchanged montmorillonite [49]. It shows the 001 reflection at 7.01° 2θ, corresponding to a basal spacing, d_{001}, of 12.6 Å. For Fe-M the 0 0 1 reflection is less intense and appears at a slightly higher angle, around 7.42° 2θ, corresponding to a lower basal space d_{001} of 12.05 Å. This result is in agreement with the differences in sizes of iron and sodium ions in their hydrated form [50], suggesting that a least part of the Fe(III) is present in the interlayer space [31]. The XRD pattern of Fe-M-P is almost coincident with that of Fe-M, and the basal spacing is not modified by the presence of phosphate. This suggests that phosphate is not entering the interlayer space and that phosphate adsorption takes place mainly on the outer surface of Fe-M particles.

Fig. 3 shows the EM vs. pH curves of the studied samples in 0.01 M NaCl solutions. The three samples show rather similar behavior, with the EM always negative between pH 3 and 9. The behavior of Na-M is well known [51–54], and it is the result of the presence of structural negative charges within the clay lattice. Fe-M has electrophoretic mobilities that are slightly less negative than those of Na-M, indicating that the presence of interlayer/sorbed Fe(III) species does not produce a strong modification in EM. On the other hand, the presence of phosphate increases slightly the negative EM of Fe-M. The fact that phosphate adsorbs significantly on Fe-M and that this adsorption produces an increase in the negative EM of the solid indicates that adsorption is not driven by electrostatic interactions. The net electrostatic repulsion between Fe-M and phosphate species seems to be overcome by some kind of specific interaction, possibly the formation of inner-sphere surface complexes between phosphate and Fe(III) species. Furthermore, the similarities in the general adsorption behavior of phosphate on Fe-M, goethite and ferrihydrite particles strongly suggest the

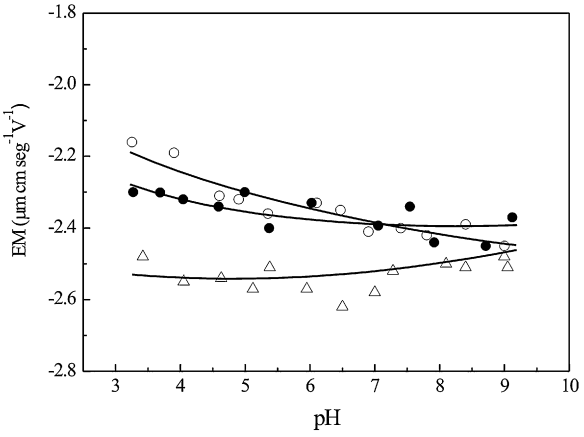

Fig. 3. Electrophoretic mobilities (EM) of Na-M (solid circles), Fe-M (open circles) and Fe-M-P (open triangles) samples in 0.01 M NaCl. Lines are drawn only to serve as guides to the eyes.

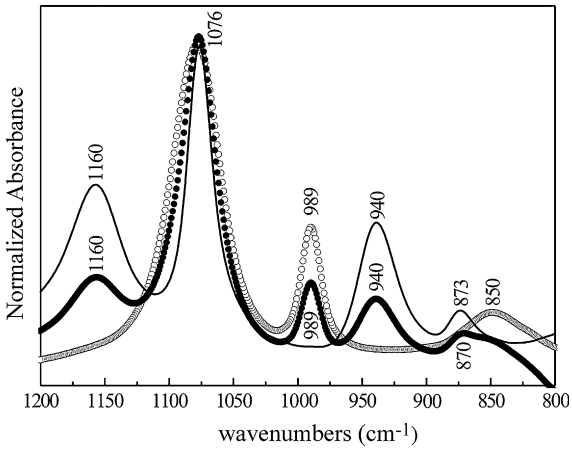

Fig. 4. ATR-FTIR spectra of phosphate species in solution at pH 4.5 (solid line), 7.0 (solid circles) and pH 9.0 (open circles).

formation of the same kind of surface complexes on the three solids. These are known to be inner-sphere complexes for the cases of goethite and ferrihydrite [19,21,22]. Consequently, the macroscopic adsorption data points to the existence of inner-sphere surface complexes of phosphate on Fe-M. However, it is difficult to ensure this existence only based on macroscopic data; hence, ATR-FTIR spectroscopic analysis is mandatory to gain insight into phosphate surface speciation at the Fe-M aqueous solution interface.

4.2. ATR-FTIR analysis

In order to evaluate the phosphate speciation at the Fe-M aqueous solution interface, the IR spectra of the adsorbed species were compared to the spectra of the phosphate species in solution at the same pH. This comparison allows distinguishing inner from outer-sphere surface complexes based on the number of vibration bands and splitting of a particular band. Both spectral features are related to the symmetry of a given species either in solution or at the interface [21,23,55].

Fig. 4 shows the ATR-FTIR spectra of phosphate species in solution at pH 4.5, 7.0 and 9.0 and Table 1 collects the observed vibration bands. At pH 4.5, the predominant species is $H_2PO_4^-$ (C_{2V} symmetry) that presents four vibration bands. Three of them (1160, 1076 and, 940 cm^{-1}) are assigned to the ν_3 asymmetric vibration split (related to ν_{as}(P–O), ν_s(P–O) and ν_{as}(P–OH) vibration bands), while the 873 cm^{-1} one is the ν_1 vibration band (ν_s(P–OH) vibration band) [20]. On the other hand, HPO_4^{2-} (C_{3V} symmetry) is the main species in solution at pH 9.0 whose spectrum shows only three bands at 1078, 989 and 850 cm^{-1} (corresponding to ν_{as}(P–O), ν_s(P–O) and ν(P–OH) vibration bands). The reduction in the number of bands, related to the increasing molecular symmetry in going from $H_2PO_4^-$ to HPO_4^{2-} [21], is assigned to the ν_3 vibration that splits into two bands (1078 and 989 cm^{-1}). The third band at 850 cm^{-1} corresponds to the ν_1 vibration as observed at pH 4.5 [21]. Since at pH 7.0 both species are present, the IR spectrum shows a combination of their vibration bands: 1160, 1076 and 940 cm^{-1} due to $H_2PO_4^-$, and 1078 and 989 cm^{-1} due to HPO_4^{2-}. The ν_1 vibration band appears at 870 cm^{-1}.

Fig. 5 shows the ATR-FTIR of phosphate adsorbed at the Fe-M aqueous solution interface. The number and position of the vibration bands (although not well resolved) depend on the pH. There are two vibration bands (at 1050 and 1080 cm^{-1}) at pH 4.5 while there is a single one (1066 cm^{-1}) at pH 7.0 and 9.0. The two bands observed at pH 4.5 may be related to the shift of the main bands (1076 and 1160 cm^{-1}) present in the spectrum of $H_2PO_4^-$ in solution. The presence of the third ν_3 vibration band belonging to the C_{2V} symmetry is obscured due to the strong absorption of the Fe-M wet film at wavenumbers below 1000 cm^{-1}, which could not be completely removed as indicated in Section 3.3.1 (see also supporting material, Note II). On the other hand, at pH 7.0 and 9.0 the single broad band may be due to the shift of the strongest ν_3

Table 1
Comparison of the peaks position obtained by FSD and second derivative method, together with (ν3) and (ν1) bands of free aqueous species of phosphate in solution at pH 4.5, 7.0 and 9.0. References are given in parenthesis.

pH 4.5							
$H_2PO_4^-$(C_{2V})	1160 (ν_3)		1076 (ν_3)			940 (ν_3)	873 (ν_1)
FSD/SD	1128/22	1088/86	1049/47	1011/16	978/80	941/44	
$(FeO)_2PO_2$ (C_{2V} or lower) [19,21,22]		1085–1096	1021–1044			945–960	
$(FeO)_2OHPO$ (C_{2V} or lower) [19]	1102–1123			1006–1012	920–982		
pH 7							
$H_2PO_4^-$/HPO_4^{2-}	1160 (ν_3)		1077 (ν_3)		989 (ν_3)	940 (ν_3)	870 (ν_1)
FSD/SD		1095/91	1062/62	1020/21	988/84	962/60	935/30
$(FeO)_2PO_2$ or $(FeO)PO_3$–H (C_{2V} or lower) [19,22,23,58]		1085–1096	1021–1044			945–960	
$(FeO)PO_3$ (C_{3V})[19]				1025–1075	990–1001		
$Co(NH3)_5PO_4$(C_{3V}) [59]				1030	980		934(ν_1)
pH 9							
HPO_4^{2-}(C_{3V})			1078 (ν_3)		989 (ν_3)		850 (ν_1)
FSD/SD		1096/96		1062/61	1023	983	957/NS	931
$(FeO)_2PO_2$ or $(FeO)PO_3$–H (C_{2V} or lower) [19,22,23,58]		1085–1096	1021–1044			945–960	
$(FeO)PO_3$ (C_{3V}) [19]				1025–1075	990–1001		
$Co(NH3)_5PO_4$(C_{3V}) [59]				1030	980		934 (ν_1)

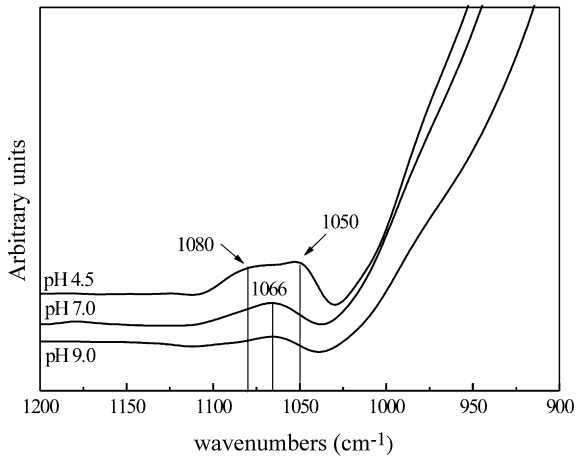

Fig. 5. ATR-FTIR spectra of phosphate adsorbed on Fe-M at pH 4.5, 7.0 and 9.0.

band (1077–1078 cm^{-1}) present in the spectra of both HPO_4^{2-} and $H_2PO_4^-$ species.

In order to achieve a better identification, the overlapped bands in the spectra of Fig. 5 were resolved by using two independent spectral analyses: SD and FSD. Both mathematical methods have been successfully applied to determine the number and positions of overlapped bands in the spectra of peptides and proteins, either in solution or adsorbed on the ATR crystal [44,45,56]. These methods were barely applied in ATR-IR studies of ion adsorption on oxide films [55], presumably because no interferences with other bands occurred. In these simpler cases, band deconvolution has been mostly performed by spectral fitting. SD and FSD spectral analyses provide a simple way of resolving overlapped bands in composite envelope as it is the case of the spectra in Fig. 5. Eventually, the number and positions of the overlapped bands found by FSD or SD may be used as initial parameters in curve-fitting routines. Due to the strong water absorption of the Fe-M wet film (wavenumbers lower than 1000 cm^{-1}), spectral fitting could not be applied to the spectra in Fig. 5. Therefore, SD and FSD were independently applied in the 1200–1900 cm^{-1} range and the spectral analyses were mainly focused on the number and positions of the ν_3 vibration bands.

For comparison purposes, Fig. 6 shows the SD and FSD analyses on the spectra of phosphate species in solution and adsorbed at pH 4.5, and Table 1 collects the number of bands and their positions. Both methods provide the same information: there are three resolved bands in solution and six in the adsorbed state. For data in solution, the number of bands and their positions coincide with the resolved bands present in the spectrum in Fig. 4, giving reliability to the spectral SD and FSD analyses.

For the case of Fe-M in the presence of phosphate, the six bands resolved at pH 4.5 correspond to adsorbed phosphate species, since these bands do not appear in absence of phosphate (see Supporting Material, Note III). They correspond to two surface complexes with C_{2V} symmetry (as the species $H_2PO_4^-$ in solution) or lower. Based on the results reported by Tejedor-Tejedor and Anderson [19], Arai and Sparks [21], Luengo et al. [22], and Elzinga and Sparks [23] (see Table 1), these bands are divided into two groups: (a) 941, 1049 and 1088 cm^{-1} and (b) 978, 1011 and 1128 cm^{-1}. The first group accounts for the main bands observed in the spectrum of Fig. 5, related to the shifted $H_2PO_4^-$ ν_3 vibrations, indicating inner-sphere surface complexes. These bands correspond to a nonprotonated bidentate complex $(FeO)_2PO_2$. On the same basis, the second group is assigned to the monoprotonated bidentate complex $(FeO)_2(OH)PO$. It is worth mentioning that Rahnemaie et al. [57] combining surface complexation modeling, FTIR data

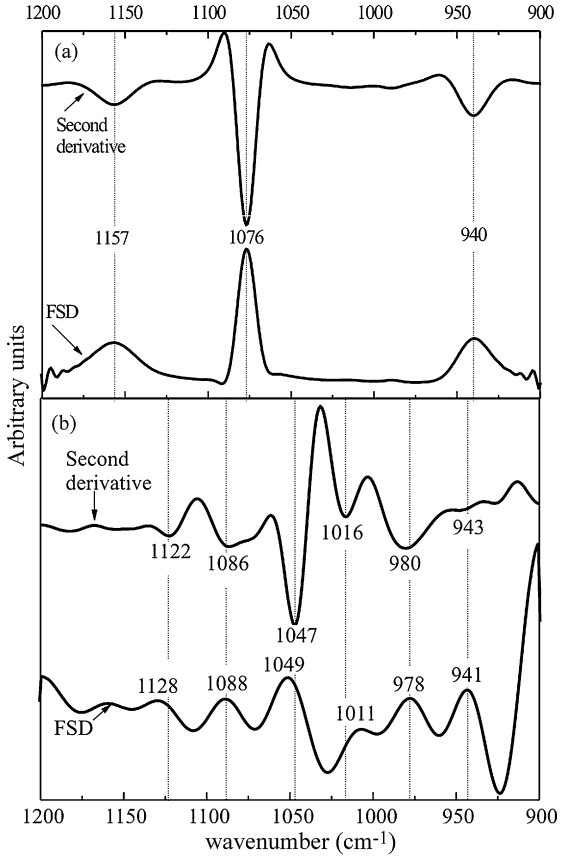

Fig. 6. Second derivative (SD) and Fourier self-deconvolution (FSD) analyses of phosphate (a) in solution and (b) adsorbed on Fe-M at pH 4.5.

and molecular calculations from the literature [19,58] assigned this band position to a protonated monodentate surface complex instead of the protonated bidentate.

Fig. 7 shows the FSD analysis performed on the spectra of the adsorbed species at the three studied pH, and Table 1 gives the positions found with FSD and SD. The spectral analyses performed at pH 7.0–9.0 also give six vibration bands that are divided as well into two groups: (a) 962–957, 1062–1062 and 1095–1096 cm^{-1}, and (b) 935–931, 988–983 and 1020–1023 cm^{-1}. The three ν_3 vibration bands of the first group are slightly shifted when compared to the same group at pH 4.5, and suggest also the presence of the $(FeO)_2PO_2$ surface group at these pH values. The slight shift in band

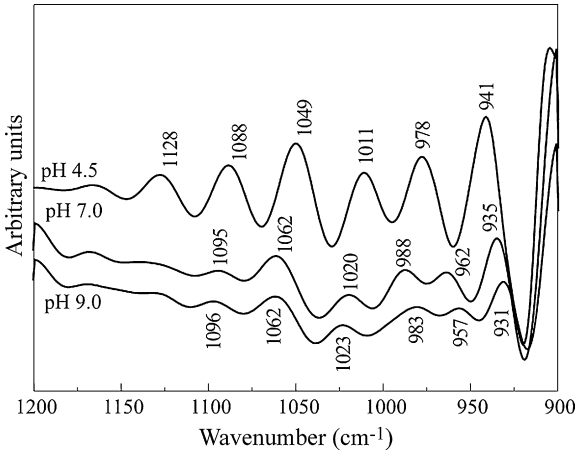

Fig. 7. Fourier self-deconvolution (FSD) analysis of phosphate adsorbed on Fe-M at pH 4.5, 7.0 and 9.0.

positions may be due to hydrogen-bonding of phosphate species to adjacent surface sites that would lead to a surface coordination that is intermediate between monodentate and bidentate ($(FeO)_2PO_2$ or $(FeO)PO_3$–H), as postulated by Elzinga and Sparks [23]. The binuclear complex is preferred at low pH and high surface coverage (weak hydrogen bond) whereas at high pH and low surface coverage the hydrogen bond to an adjacent surface is favored promoting monodentate mononuclear complexes. Since both surface complexes have C_{2V} symmetry or lower, the interpretation of the IR spectra is ambiguous [58].

The three vibration bands (935, 988 and 1020 cm^{-1}) of the second group were assigned following the IR spectrum of the monodentate mononuclear $Co(NH_3)_5PO_4$ complex, previously used as a reference compound with C_{3v} symmetry [59]. Two (1020 and 988 cm^{-1}) of the three bands in the spectra correspond to the ν_3 vibration split and the one centered at 935 cm^{-1} is related to the ν_1 band, as already discussed for the C_{3v} HPO_4^{2-} species in solution. On this basis, the spectral analyses of the adsorbed phosphate on Fe-M indicate the presence of a surface complex with C_{3V} symmetry at pH 7.0 and 9.0. The positions of the ν_3 vibration bands (988 and 1020 cm^{-1}) are similar to those found by Tejedor-Tejedor and Anderson [19] (1001 and 1025 cm^{-1}) which were assigned to a nonprotonated monodentate complex ($(FeO)PO_3$). The ν_3 vibration bands, related to the $\nu(PO_3)$ mode of the surface complex are expected to be at lower wavenumbers than those of the HPO_4^{-} species in solution (1076–1078 and 989 cm^{-1}) because metal ions are not as strongly coordinated to oxygen ions as proton [19]. Moreover, the ν_1 vibration band, accounting for the ν(POM) mode, of the surface complex is likely to be at higher wavenumbers than the counterpart in solution (850 cm^{-1}), as observed in the spectra of Fig. 7.

The ATR-FTIR spectral analyses reveal the existence of inner-sphere complexes when phosphate adsorbs on Fe-M as already suggested from macroscopic adsorption data and electrophoresis. The identified surface complexes have been also found in other IR studies reporting the adsorption of phosphate on different Fe(III) (hydr)oxides [19–23]. These complexes were also proposed by several authors when modeling the adsorption of phosphate on goethite [3,17]. The similarity in the type of surfaces complexes when either goethite, Fe(III) (hydr)oxides or Fe-M interacts with phosphate also indicates that phosphate is mainly attached to Fe(III) (hydr)oxide coatings in Fe-M.

5. Conclusions

The applied ATR-FTIR spectral analyses allow to evaluate the phosphate speciation at the Fe(III) modified montomorillonite-aqueous solution interface. Phosphate forms inner-sphere surface complexes when adsorbed on Fe-M particles with a coordination that depends on the pH. At pH 4.5, two surface complexes with C_{2V} symmetry or lower are formed: nonprotonated bidentate ($(FeO)_2PO_2$) and monoprotonated bidentate ($(FeO)_2OHPO$). On the other hand, the two surface complexes at pH 7.0 and 9.0 present C_{2V} or lower and C_{3V} symmetry. These inner-sphere surface complexes are identified as nonprotonated bidentate and nonprotonated monodentate ($(FeO)_2PO_2$ or $(FeO)PO_3$–H) and ($(FeO)PO_3$). All of them are not associated with montmorillonite itself but with the Fe(III) (hydr)oxides coatings. Therefore, the clay acts as a carrier or support of the Fe(III) (hydr)oxides, and these coatings are responsible for phosphate adsorption.

Acknowledgments

The authors thank the Consejo Nacional de Investigaciones Científicas y Técnicas de Argentina (CONICET), FONCyT, SECyT-UNC and SeCyT-UNS for financial support. L.B thanks CONICET for the fellowship granted. Thanks are also due to Dra. Laura Valenti for the assistance in interpreting IR spectra.

Appendix A. Supplementary data

Supplementary data associated with this article can be found, in the online version, at doi:10.1016/j.colsurfa.2009.11.022.

References

[1] O.R. Harvey, R.D. Rhue, Kinetics and energetics of phosphate sorption in a multicomponent Al(III)–Fe(III) hydr(oxide) sorbent system, J. Colloid Interface Sci. 322 (2008) 384–393.
[2] C. Spiteri, P. Van Capellen, P. Regnier, Surface complexation effects on phosphate adsorption to ferric iron oxyhydroxides along pH and salinity gradients in estuaries and coastal aquifers, Geochim. Cosmochim. Acta 72 (2008) 3431–3445.
[3] J. Antelo, M. Avena, S. Fiol, R. López, F. Arce, Effect of phosphate and ionic strength on the adsorption of phosphate and arsenate at the goethite-water interface, J. Colloid Interface Sci. 285 (2005) 476–486.
[4] L. Borgnino, C. Orona, M. Avena, A. Maine, A. Rodríguez, C.P. De Pauli, Phosphate concentration an association as revealed by sequential extraction and microprobe analysis: the case of two Argentinean reservoirs, Water Resour. Res. 42 (2006) W01414, doi:101029/2005WR004031.
[5] L. Borgnino, M. Avena, C.P. De Pauli, Surface properties of sediments from two Argentinean reservoirs and the rate of phosphate release, Water Res. 40 (2006) 2659–2666.
[6] H. Klapper, Control of Eutrophication in Inland Waters, Ellis Horwood, Chichester, 1991.
[7] P.J.A. Withers, H.P. Jarvie, Delivery and cycling of phosphorus in rivers: a review, Sci. Total Environ. 400 (2008) 379–395.
[8] J.E. Vermaat, A. Mc Quatters-Gollop, M.A. Eleveld, A.J. Gilbert, Past, present and future nutrient loads of the North Sea: causes and consequences Estuarine, Coast. Shelf Sci. 80 (2008) 53–59.
[9] B.M. Spears, L. Carvalho, R. Perkins, A. Kirika, D.M. Paterson, Spatial and historical variation in sediment phosphorus fractions and mobility in a large shallow lake, Water Res. 40 (2006) 383–391.
[10] L. Sigg, W. Stumm, The interaction of anions and weak acids with the hydrous goethite (α-FeOOH) surface, Colloid Surf. 2 (1981) 101–117.
[11] N. Nilsson, P. Persson, L. Lovgren, S. Sjoberg, Competitive surface complexation of o-phthalate and phosphate on goethite (α-FeOOH) particles, Geochim. Cosmochim. Acta 60 (1996) 4385–4395.
[12] J.S. Geelhoed, T. Hiemstra, W.H. van Riemsdijk, Phosphate and sulfate adsorption on goethite: single anion and competitive adsorption, Geochim. Cosmochim. Acta 61 (1997) 2389–2396.
[13] R.P.J.J. Rietra, T. Hiemstra, W.H. van Riemsdijk, Interaction between calcium and phosphate adsorption on goethite, Environ. Sci. Technol. 35 (2001) 3369–3374.
[14] H. Zhao, R. Stanforth, Competitive adsorption of phosphate and arsenate on goethite, Environ. Sci. Technol. 35 (2001) 4753–4757.
[15] J. Antelo, F. Arce, M.J. Avena, S. Fiol, R. López, F. Macías, Adsorption of a soil humic acid at the surface of goethite and its competitive interaction with phosphate, Geoderma 138 (2007) 12–19.
[16] B.A. Manning, S. Goldberg, Modeling competitive adsorption of arsenate with phosphate and molybdate on oxide minerals, Soil Sci. Soc. Am. J. 60 (1996) 121–131.
[17] T. Hiemstra, W.H. van Riemsdijk, A surface structural approach to ion adsorption: the charge distribution (CD) model, J. Colloid Interface Sci. 179 (1996) 488–508.
[18] T. Hiemstra, van Riemsdijk W.H., Surface structural ion adsorption modeling of competitive binding of oxyanions by metal (hydr)oxides, J. Colloid Interface Sci. 210 (1999) 182–193.
[19] M.I. Tejedor-Tejedor, M.A. Anderson, Protonation of phosphate on the surface goethite as studied by CIR-FTIR and electrophoretic mobility, Langmuir 6 (1990) 602–611.
[20] P. Persson, N. Nilsson, S. Sjöberg, Structure and bonding of orthophosphate ions at the iron oxide-aqueous interface, J. Colloid Interface Sci. 177 (1996) 263–275.
[21] Y. Arai, D. Sparks, ATR-FTIR spectroscopy investigation on phosphate adsorption mechanism at the ferrihydrite-water interface, J. Colloid Interface Sci. 241 (2001) 317–326.
[22] C. Luengo, M. Brigante, J. Antelo, M. Avena, Kinetic of phosphate adsorption on goethite: comparing batch adsorption and ATR-IR measurements, J. Colloid Interface Sci. 300 (2006) 511–518.
[23] E.J. Elzinga, D. Sparks, Phosphate adsorption onto hematite: An in situ ATR-FTIR investigation of the effects of pH and loading level on the mode of phosphate surface complexation, J. Colloid Interface Sci. 308 (2007) 53–70.
[24] N. Khare, J.D. Martin, D. Hesterberg, Phosphate bonding configuration on ferrihydrite based on molecular orbital calculations and XANES fingerprinting, Geochim. Cosmochim. Acta 71 (2007) 4405–4415.
[25] T. Hou, R. Xu, D. Tiwari, A. Zhao, Interaction between electrical double layers of soil colloids and Fe/Al oxides in suspensions, J. Colloid Interface Sci. 310 (2007) 670–674.

[26] Y. Xu, L. Axe, Synthesis and characterization of iron oxide-coated silica and its effect on metal adsorption, J. Colloid Interface Sci. 282 (2005) 11–19.
[27] V. Lenoble, O. Bouras, V. Deluchat, B. Serpaud, J.C. Bollinger, Arsenic adsorption onto pillared clays and iron oxides, J. Colloid Interface Sci. 3255 (2002) 52–58.
[28] D. Karamaris, P.A. Asimakopoulos, Efficiency of aluminum-pillared montmorillonite on the removal of cesium and copper from aqueous solutions, Water Res. 41 (2007) 1897–1906.
[29] T. Undabeytia, S. Nir, T. Sánchez-Verdejo, J. Villaverde, C. Maqueda, E. Morillo, A clay–vesicle system for water purification from organic pollutants, Water Res. 42 (2008) 1211–1219.
[30] M.P.F. Fontes, S.B. Weed, Phosphate adsorption by clays from Brazilian oxisols: relationship with specific surface area and mineralogy, Geoderma 72 (1996) 37–51.
[31] L. Borgnino, M. Avena, C.P. De Pauli, Synthesis and characterization of Fe(III)-montmorillonites for phosphate adsorption, Colloids Surf. A: Physicochem. Eng. Aspects 341 (2009) 46–52.
[32] T. Kasama, Y. Watanabe, H. Yamada, T. Murakami, Sorption of phosphates on Al-pillared smectites and mica at acidic to neutral pH, Appl. Clay Sci. 25 (2004) 167–177.
[33] M.-X. Zhu, K.-Y. Ding, S.-H. Xu, X. Jiang, Adsorption of phosphate on hydroxyaluminum- and hydroxyiron-montmorillonite complexes, J. Hazard. Mater. 165 (2008) 645–651.
[34] B.B. Yosef, U. Kafkari, R. Rosenberg, G. Sposito, Phosphorous adsorption by kaolinite and montmorillonite. I. Effect of time, ionic strength and pH, Soil Sci. Soc. Am. J. 52 (1988) 1580–1585.
[35] J. Zhuang, G.-R. Yu, Effects of surface coating on electrochemical properties and contaminant sorption of clay minerals, Chemosphere 49 (2002) 619–628.
[36] A.A. Jara, S. Goldberg, M.L. Mora, Studies of the charge of amorphous aluminosilicates using surface complexation models, J. Colloid Interface Sci. 292 (2005) 160–170.
[37] I. Carabante, M. Grahn, A. Holmgren, J. Kumpiene, J. Hedlund, Adsorption of As (V) on iron oxide nanoparticle films studied by in situ ATR-FTIR spectroscopy, Colloids Surf. A: Physicochem. Eng. Aspects 346 (2009) 106–113.
[38] G. Lefèvre, In situ Fourier-transform infrared spectroscopy studies of inorganic ions adsorption on metal oxides and hydroxides, Adv. Colloid Interface Sci. 107 (2003) 109–123.
[39] M.J. Avena, L. Valenti, V. Pfaffen, C.P. De Pauli, Methylene blue dimerization does not interference in surface-area measurements of kaolinite and soils, Clays Clay Miner. 49 (2001) 168–173.
[40] J. Murphy, J.P. Riley, A modified single solution method for determination of phosphate in natural waters, Anal. Chem. 27 (1962) 31–36.
[41] L. Yan, C.B. Roth, P.F. Low, Changes in the Si–O vibrations of smectites layers accompanying the sorption of interlayer water, Langmuir 12 (1996) 4421.
[42] C.T. Johnston, G.S. Premachanda, Polarized ATR-FTIR study of smectite in aqueous suspension, Langmuir 17 (2001) 3712–3718.
[43] P.B. Tooke, Fourier self-deconvolution in IR spectroscopy, TrAC Trends Anal. Chem. 7 (1988) 130–136.
[44] S.-Y. Lin, T.-F. Hsieh, Y.-S. Wei, pH and thermal-dependent conformational transition of PGAlPG, a repeated hexapeptide sequence from tropoelastin, Peptides 26 (2005) 543–549.
[45] J. Zhang, Y.-B. Yang, Probing conformational changes of proteins by quantitative second-derivative infrared spectroscopy, Anal. Biochem. 340 (2005) 89–98.
[46] M.A. Anderson, M.I. Tejedor-Tejedor, R.R. Stanforth, Influence of aggregation on the uptake kinetics of phosphate by goethite, Environ. Sci. Technol. 19 (1985) 632–637.
[47] A. Jain, K. Raven, R.H. Loeppert, Arsenite and arsenate adsorption on ferrihydrite: surface charge reduction and net OH– release stoichiometry, Environ. Sci. Technol. 33 (1999) 1179–1184.
[48] H.S. Zhao, R. Stanforth, Competitive adsorption of phosphate and arsenate on goethite, Environ. Sci. Technol. 35 (2001) 4753–4757.
[49] H. Dramé, Cation exchange and pillaring of smectites by aqueous Fe nitrate solutions, Clays Clay Miner. 53 (2005) 335–347.
[50] D. Richens, The chemistry of Aqua Ions, John Wiley & Sons, Chichester, 1997.
[51] S.E. Miller, P.F. Low, Characterization of the electrical double layer of montmorillonite, Langmuir 6 (1990) 572–578.
[52] M.J. Avena, C.P. De Pauli, Proton adsorption and electrokinetics of an Argentinean montmorillonite, J. Colloid Interface Sci. 202 (1998) 195–204.
[53] F. Thomas, L.J. Michot, D. Vantelon, E. Montargès, B. Prélot, M. Cruchaudet, J.F. Delon, Layer charge and electrophoretic mobility of smectites, Colloids Surf. A: Physicochem. Eng. Aspects 159 (1999) 351–358.
[54] M.J. Avena, Acid-base behavior of clay surfaces in aqueous media, in: P. Somasundaran, Dekker Marcel (Eds.), Encyclopedia of Surface and Colloid Science, New York, 2006, pp. 17–46.
[55] W. Gong, A real time in situ ATR-FTIR spectroscopic study of linear phosphate adsorption on titania surfaces, J. Miner. Process. 63 (2001) 147–165.
[56] C.E. Giacomelli, M.G.E.G. Bremer, W. Norde, ATR-FTIR, Study of IgG adsorbed on different silica surfaces, J. Colloid Interface Sci. 220 (1999) 13–23.
[57] R. Rahnemaie, T. Hiemstra, W.H. van Riemsdijk, Geometry, charge distribution, and surface speciation of phosphate on goethite, Langmuir 23 (2007) 3680–3689.
[58] K. Kwon, J.D. Kubicki, Molecular orbital theory study on surface complex structures of phosphates to iron hydroxides: calculation of vibrational frequencies and adsorption energies, Langmuir 20 (2004) 9249–9254.
[59] R.J. Atkinson, R.L. Parfitt, R.S. Smart, Infra-red study of phosphate adsorption on goethite, J. Chem. Soc. Faraday Trans. 70 (1974) 1479.